Article

Discovery Medicine 2026; 38(207): 1054–1063
https://doi.org/10.24976/Discov.Med.202638207.84

Prophylactic PEPITEM Administration Reduces Expression of Chemokine Signaling and T-cell Migration Genes in Experimental Autoimmune Encephalomyelitis Model: RT^2 Profiler™ PCR Arrays

Mohammed Alassiri[1,2], Aiman Saud Alhazmi[1,2], Fahd Al Sufiani[2], Bahauddeen M. Alrfaei[3,4], Hasan Alnakhli[2], Mohammed Alasseiri[5], Abdullah Alamri[6], Jilani Shaik[6], Mohammad Alanazi[6], Mashan L. Abdullah[7,*]

[1]Department of Basic Sciences, College of Science and Health Professions, King Saud Bin Abdulaziz University for Health Sciences (KSAU-HS), King Abdullah International Medical Research Center (KAIMRC), 11481 Riyadh, Saudi Arabia
[2]Department of Pathology and Laboratory Medicine, King Abdulaziz Medical City (KAMC), Ministry of National Guard-Health Affairs (MNGHA), 11481 Riyadh, Saudi Arabia
[3]Department of Basic Medical Sciences, College of Medicine, King Saud Bin Abdulaziz University for Health Sciences (KSAU-HS), King Abdullah International Medical Research Center (KAIMRC), King Abdulaziz Medical City (KAMC), 11481 Riyadh, Saudi Arabia
[4]Department of Cellular Therapy and Cancer Research, King Abdullah International Medical Research Center (KAIMRC), King Saud Bin Abdulaziz University for Health Sciences (KSAU-HS), Ministry of National Guard-Health Affairs (MNGHA), 11481 Riyadh, Saudi Arabia
[5]Department of Medical Laboratory Technology, Faculty of Applied Medical Sciences, University of Tabuk, 47512 Tabuk, Saudi Arabia
[6]Genome Research Chair, Department of Biochemistry, College of Science, King Saud University, 11451 Riyadh, Saudi Arabia
[7]Department of Experimental Medicine, King Abdullah International Medical Research Center (KAIMRC), King Saud Bin Abdulaziz University for Health Sciences (KSAU-HS), Ministry of National Guard-Health Affairs (MNGHA), 11481 Riyadh, Saudi Arabia
*Correspondence: aldlamyme@ngha.med.sa (Mashan L. Abdullah)
Submitted: 13 November 2025 Revised: 5 December 2025 Accepted: 25 December 2025 Published: 20 April 2026

Background: Multiple sclerosis (MS) is a chronic autoimmune disorder of the central nervous system, characterized by inflammation, demyelination, and neurodegeneration. Experimental autoimmune encephalomyelitis (EAE) is a well-established preclinical model for examining MS pathophysiology. Peptide inhibitor of transendothelial migration (PEPITEM) is an immunomodulatory peptide; however, its effects on gene expression in EAE remain insufficiently characterized. In this study, we aimed to evaluate the immunomodulatory effects of PEPITEM in EAE by comparing therapeutic (postinduction) and prophylactic (preinduction) administration using RT^2 Profiler™ PCR Array–based gene expression analysis.

Methods: Ten female C57BL/6 mice aged 9–13 weeks (body weight, 21 $\pm$ 3 g) were induced with EAE and assigned to four experimental groups: G1 (EAE + scramble peptide), G2 (EAE + PEPITEM), G3 (EAE + scramble peptide administered preinduction), and G4 (EAE + PEPITEM administered preinduction). Gene expression was assessed using RT^2 Profiler™ PCR Arrays, with fold regulation calculated for each gene.

Results: PEPITEM exerted distinct, time-dependent effects on immune gene expression. Therapeutic administration (G2 vs. G1) resulted in broad upregulation of immune-related genes, with notable increases in motif chemokine ligand 11 (*Cxcl11*) (30.14-fold), *Cd28* (3.83-fold), and *Cd40* (3.81-fold), consistent with enhanced expression of genes associated with T-cell costimulation, cytokine signaling, and chemokine signaling. Conversely, prophylactic administration (G4 vs. G3) produced marked suppression of inflammatory gene expression, with 33 of 34 genes downregulated. The most strongly suppressed genes were motif chemokine ligand 10 (*Cxcl10*) (–17.11-fold), interferon-gamma (*Ifng*) (–13.12-fold), and tumor necrosis factor-alpha (*Tnf*) (–12.43-fold), indicating reduced expression of genes involved in chemokine signaling and T-cell migration.

Conclusion: PEPITEM modulates immune-related gene expression in EAE in a timing-dependent manner. Its opposing effects—gene expression activation postinduction and suppression preinduction—suggest context-specific immunomodulatory properties that may be relevant to therapeutic strategies for MS.

Keywords: multiple sclerosis; PEPITEM; experimental autoimmune encephalomyelitis; inflammation; PCR arrays

Introduction

Multiple sclerosis (MS) is an autoimmune, inflammatory disorder of the central nervous system (CNS) characterized by demyelination, axonal damage, and neurodegeneration. The disease is primarily driven by autoreactive T cells, particularly Th1 and Th17 subsets, which infiltrate the CNS, trigger local inflammation, and mediate myelin damage [1,2]. The experimental autoimmune encephalomyelitis (EAE) model is extensively used to examine MS pathophysiology and to evaluate potential therapeutic interventions [3]. Although immunomodulatory therapies—such as interferon-β, fingolimod, and monoclonal antibodies have improved MS management, they primarily target disease progression rather than its initiation and are often associated with adverse effects arising from broad immunosuppression [4,5]. Identifying novel therapeutic strategies that precisely modulate pathogenic inflammatory pathways while preserving essential immune regulation remains a central objective in MS research.

Peptide inhibitor of transendothelial migration (PEPITEM), a naturally occurring peptide, has emerged as a potential modulator of immune responses by regulating immune cell migration and inflammatory signaling pathways [6,7]. Previous studies indicate that PEPITEM may affect monocyte and lymphocyte trafficking, cytokine interactions, and endothelial cell activation, all of which are key processes in MS pathogenesis [8–10]. Nevertheless, the effects of PEPITEM treatment in EAE remain insufficiently characterized, particularly regarding its impact on immune-related gene expression [11]. Given that immune modulation in MS can vary significantly depending on the timing of intervention, it is essential to determine whether PEPITEM exerts distinct effects when administered therapeutically (postinduction) versus prophylactically (preinduction).

Several key genes and pathways play central roles in the pathogenesis of MS and EAE by regulating immune activation, neuroinflammation, and disease progression. Chemokines, including *Cxcl10* and *Cxcl11*, regulate the recruitment of immune cells—particularly T cells and monocytes—into the CNS, thereby exacerbating inflammation and promoting demyelination [12,13]. Cytokines, such as interferon-gamma (*Ifng*) and tumor necrosis factor-alpha (*Tnf*), drive Th1- and Th17-mediated neuroinflammation, resulting in blood–brain barrier disruption and enhanced immune cell infiltration [14]. Costimulatory molecules, such as *Cd28* and *Cd40*, are critical for T-cell activation and antigen presentation, shaping the immune response and influencing disease severity [15]. Additionally, chemokine receptors, such as *Cxcr3*, mediate T-cell migration into inflamed CNS tissues, amplifying neuroinflammation [16,17]. Dysregulation of these genes and their associated pathways plays a pivotal role in EAE progression, influencing both the initiation of the immune response and the extent of neuroinflammatory damage; therefore, they represent key targets for therapeutic interventions.

The aim of this study was to examine the differential effects of PEPITEM treatment in EAE, with a specific focus on its impact on immune-related gene expression and inflammatory pathways using RT^2 Profiler™ PCR Arrays. By comparing the therapeutic and prophylactic administration of PEPITEM, we sought to determine how the peptide modulates key inflammatory and immunoregulatory pathways in EAE. Understanding the timing-dependent effects of PEPITEM on gene expression may provide valuable insights into its potential as a therapeutic or preventive strategy for MS.

Materials and Methods

Reagents

EAE induction kits were obtained from Hooke Laboratories (Cat. No. EK-2110; Hooke Laboratories, LLC, USA) and included prefilled syringes containing myelin oligodendrocyte glycoprotein 35–55 ($MOG_{35–55}$) emulsified in complete Freund's adjuvant, as well as vials of pertussis toxin (PTX) in glycerol buffer. For RNA isolation and gene expression analysis, the following kits and reagents were used: RT^2 First Strand Kit (Cat. No. 330404), RT^2 SYBR Green qPCR Mastermix (Cat. No. 330523), RNeasy Plus Universal Mini Kit (Cat. No. 73404), and the RT^2 Profiler™ PCR Array Mouse Multiple Sclerosis (GeneGlobe ID: PAMM-125ZA-2; Cat. No. 330231), all purchased from Qiagen (Hilden, Germany).

PEPITEM (Ref. 14873A) and scrambled peptide (Ref. A4960-2) were synthesized and purified using Thermo Fisher Scientific (Waltham, MA, USA), as previously described [8]. All reagents were prepared according to the manufacturer's protocols and as detailed in previous publications [18]. Mice were maintained in a pathogen-free facility with free access to food and water. All experimental procedures were conducted in accordance with institutional ethical guidelines and approved by the relevant animal ethics committee.

Study Design and Experimental Groups

This study constitutes a predefined subanalysis of a larger experimental EAE study previously reported [8]. In the parent study, 10 9–13-week-old female C57BL/6 mice (21 $\pm$ 3 g) were randomly assigned to each of four experimental groups, with each group further divided into two subcohorts: five mice were allocated for fixed-tissue collection for histology and immunohistochemistry, and five mice were allocated for frozen-tissue collection for molecular analyses. In the present study, a subset of three mice per group from the frozen-tissue cohort was used for molecular analysis. EAE was induced using $MOG_{35–55}$ peptide (100 µg) emulsified in complete Freund's adjuvant supplemented with 5 mg/mL Mycobacterium tuberculosis, fol-

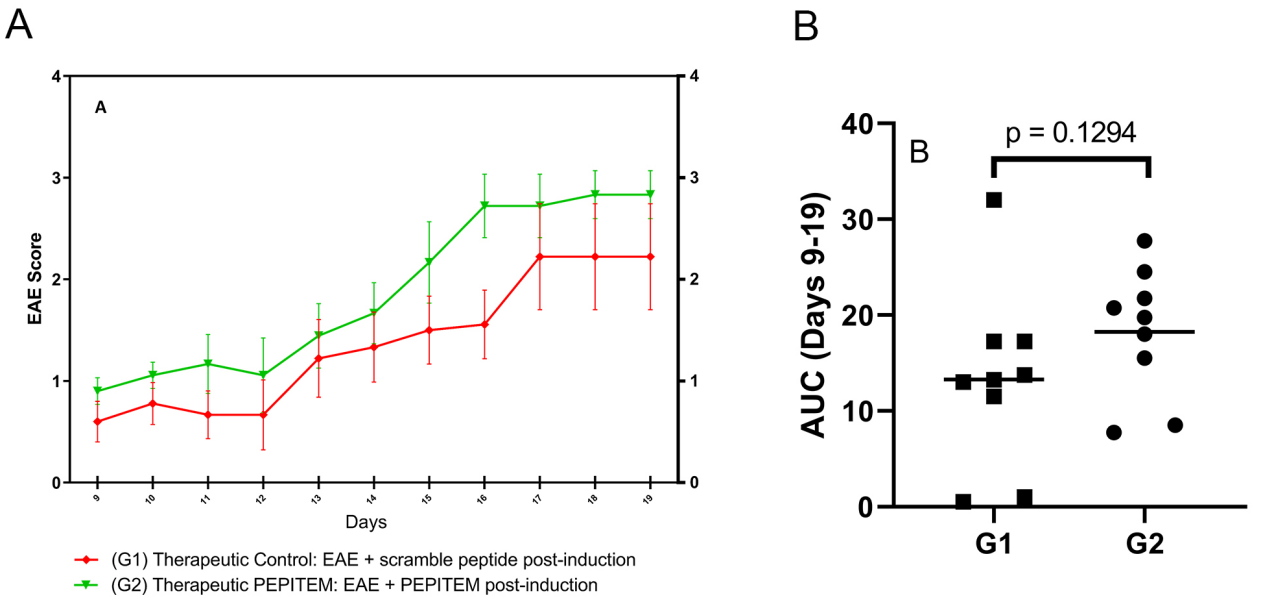

Fig. 1. Therapeutic effects of peptide inhibitor of transendothelial migration (PEPITEM) on daily experimental autoimmune encephalomyelitis (EAE) progression. (A) Daily progression of EAE clinical scores under the therapeutic protocol. The graph depicts the evolution of EAE scores over time in two experimental groups: control (G1, red) and PEPITEM-treated (G2, green). The vertical axis represents the EAE clinical score, reflecting disease severity on a standardized scale from 0 (no observable symptoms) to 5 (severe paralysis), while the horizontal axis indicates the number of days postinduction. Data points represent the mean EAE score for each group at the corresponding time point, illustrating the overall disease course and differences in progression between the groups. Data analysis and graphical representation were performed using GraphPad Prism software. (B) Cumulative disease burden assessed by area under the curve (AUC) analysis. The AUC of the clinical score was calculated for each mouse using the trapezoidal rule over the observation period (days 9–19). AUC values were compared between groups using a two-tailed Mann–Whitney U test in GraphPad Prism. No statistically significant difference was observed between the groups ($p = 0.1294$; n = 9). Two mice per group were excluded from the analysis and euthanized due to the absence of clinical disease development by day 11 postinduction.

lowed by PTX (200 ng) administration on days 0 and 2. Mice that did not exhibit clinical signs of EAE within 10 ± 1 d from the start of the experiment were excluded and humanely euthanized. Mice were assigned to the following groups: (G1) Therapeutic Control: EAE + scramble peptide postinduction, (G2) Therapeutic PEPITEM: EAE + PEPITEM postinduction, (G3) Prophylactic Control: EAE + scramble peptide preinduction, and (G4) Prophylactic PEPITEM: EAE + PEPITEM preinduction. Daily intraperitoneal injections commenced on day 10 ± 1 for postinduction groups, corresponding to the onset of initial clinical signs, and on day 1 for the preinduction groups, continuing until day 21. PEPITEM was administered at a concentration of 100 mg/mL in a total volume of 200 µL per injection, following the protocol established in our previous studies [6,7]. PEPITEM and the scrambled control peptide were administered through daily intraperitoneal injections, consistent with previous *in vivo* PEPITEM studies showing systemic efficacy using this route of administration.

EAE Scoring

Clinical signs of EAE were evaluated daily using the standardized 0–5 scoring scale recommended by Hooke Laboratories, as previously described [8,11]. Clinical scoring was performed by the animal caretaker and a trained member of the research team, with final scores for each mouse confirmed by the veterinarian coinvestigator. To minimize observer bias, scoring criteria were applied consistently across observers and time points using the same standardized scale and involving multiple qualified assessors. Mice were monitored daily for changes in body weight, EAE scores, behavior, clinical signs, and mortality. EAE scoring followed guidelines adapted from the Hooke Laboratories induction kit manual. Animal care personnel and research team members recorded the scores independently each day. The scoring scale was defined as follows: a score of 0 indicated no observable symptoms, 0.5 represented slight tail weakness, 1 denoted complete tail paralysis, 1.5 indicated tail paralysis accompanied by a mildly unsteady gait, 2 reflected tail paralysis with partial hind limb weakness, 2.5 corresponded to tail paralysis with clear hind

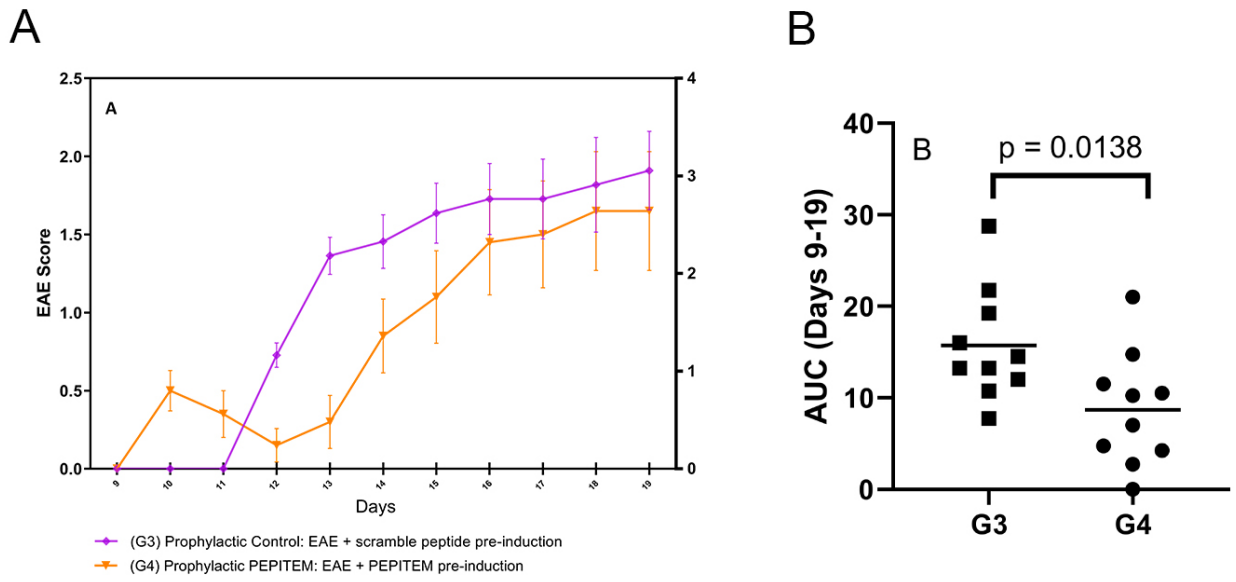

Fig. 2. Prophylactic effects of PEPITEM on daily EAE progression. (A) Daily progression of EAE clinical scores under the prophylactic protocol. The graph shows the evolution of EAE scores over time in two experimental groups: control (G3, purple) and PEPITEM-treated (G4, orange). The vertical axis represents the EAE clinical score, reflecting disease severity on a standardized scale from 0 (no observable symptoms) to 5 (severe paralysis), and the horizontal axis indicates day postinduction. Data points represent the mean EAE score for each group at the corresponding time point, indicating the overall disease course and differences in progression between the groups. Data analysis and graphical representation were performed using GraphPad Prism software. (B) Cumulative disease burden assessed by AUC analysis. The AUC of the clinical score was calculated individually for each mouse using the trapezoidal rule across the observation period (days 9–19). AUC values were compared between groups using a two-tailed Mann–Whitney *U* test in GraphPad Prism. Statistically significant differences were observed between the groups ($p = 0.0138$; n = 10).

limb weakness, 3 indicated complete paralysis of the tail and hind limbs, 3.5 was assigned when the mouse was unable to right itself when placed on its side, in addition to tail and hind limb paralysis, 4 signified additional involvement of the front limb, and a score of 5 represented total paralysis or death, at which point humane euthanasia was performed. Cumulative disease burden was assessed using area under the curve (AUC) analysis.

RNA Extraction and Gene Expression Analysis

On day 22 postinduction, mice were euthanized by overdose of inhaled isoflurane (≥5%). Death was confirmed by cessation of respiration and cardiac activity, after which thoracotomy with exsanguination was performed as a secondary method. CNS tissues, including the spinal cord and brain, were then collected. Total RNA was extracted from brain tissue using the RNeasy Mini Kit (QIAGEN) in accordance with the manufacturer's protocol. RNA concentration and purity were assessed using a NanoDrop 2000 (Thermo Fisher Scientific Inc., Wilmington, DE, USA). Complementary DNA (cDNA) synthesis was performed using the RT^2 First Strand Kit, and gene expression profiling was conducted using RT^2 Profiler™ PCR Arrays, which target key genes involved in T-cell activation, cytokine signaling, chemokine pathways, and oxidative stress responses. Real-time PCR was performed on an X-brand Applied Biosystems thermal cycler (Veriti 96-Well Thermal Cycler; Thermo Fisher Scientific, Waltham, MA, USA), and fold-regulation values were calculated using the ΔΔCt method. Gene expression levels were normalized to the housekeeping genes glyceraldehyde-3-phosphate dehydrogenase (*Gapdh*) and *β*-actin.

RT^2 Profiler™ PCR Array

Gene expression analysis was performed using the RT^2 Profiler™ PCR Array Mouse Multiple Sclerosis panel (PAMM-125Z) from Qiagen, in accordance with the manufacturer's instructions. The 96-well array plate contained primers for 84 target genes, five housekeeping genes, and three internal controls designed to monitor assay performance and improve reaction sensitivity and specificity. Following cDNA synthesis, as described above, the PCR reaction mixtures were prepared separately for each experimental condition. For each mixture, 1350 µL of RT^2 SYBR Green Master Mix, 102 µL of cDNA, and 1248 µL of RNase-free water were combined in a sterile 5 mL tube. Aliquots of 25 µL of the PCR mixtures were then dispensed into each well of the RT^2 Profiler™ PCR Array plate. The

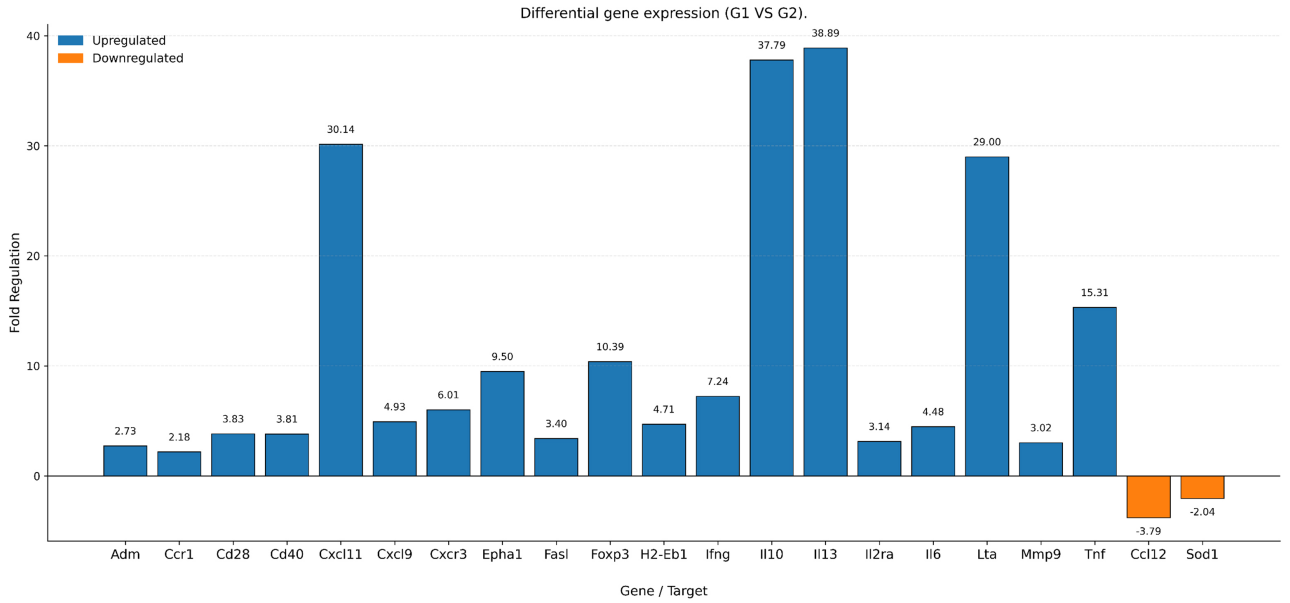

Fig. 3. Differential gene expression under therapeutic conditions (G1 vs. G2). The bar plot illustrates changes in gene expression expressed as fold regulation between the therapeutic groups G1 and G2. Positive fold regulation values indicate gene upregulation, whereas negative values indicate gene downregulation relative to the reference group. Upregulated genes are shown in blue, and downregulated genes are shown in orange. Fold regulation values were calculated using the manufacturer's ΔΔCt method. Only genes with an absolute fold regulation value of ≥2 and a *p*-value < 0.05 were considered significantly altered and are shown in the plot (n = 3).

plate was centrifuged at 1000 ×*g* for 1 min at 25 °C to remove air bubbles and ensure uniform reagent distribution. Real-time PCR amplification was subsequently performed. Relative gene expression levels were calculated using the comparative cycle threshold ($2^{-\Delta\Delta Ct}$) method, and results were expressed as fold changes relative to the control samples. Each experiment was performed in triplicate.

In Silico Analysis

A network of all associated genes was constructed to analyze gene–gene interactions. Functional associations at the protein level were predicted using GeneMANIA v3.5.3 (University of Toronto, Toronto, ON, Canada), which was used to generate a network of common genes and to identify additional functionally related genes. GeneMANIA can be accessed through the "App Manager" in Cytoscape v3.10.2 (Institute for Systems Biology, Seattle, WA, USA). The GeneMANIA network integrates multiple data types, including coexpression, predicted interactions, shared protein domains, physical interactions, and colocalization. Using the GeneMANIA algorithm with default parameters, an interconnected network of differentially regulated genes was generated, highlighting relationships based on physical interactions, coexpression, prediction, colocalization, pathway, genetic interactions, or shared protein domains. Fold-regulation values derived from RT^2 Profiler™ Array analysis were used to assess the direction and magnitude of gene expression changes, with positive values indicating upregulation and negative values indicating downregulation (using an inverse fold-change transformation). Genes with a fold regulation of ≥+2 or ≤–2 were considered meaningfully altered, whereas values between –2 and +2 were considered not significantly changed, as expression levels remained close to those of the control group.

Statistical Analysis

All experiments were performed at least three times independently. Data were analyzed using GraphPad Prism 8 (GraphPad Software Inc., La Jolla, CA, USA). Continuous variables are presented as mean ± standard deviation. Gene expression levels were determined using the $2^{-\Delta\Delta Ct}$ method and expressed as fold changes relative to the control group. For RT^2 Profiler™ PCR array data, the GeneGlobe Data Analysis Center (QIAGEN) was also employed to facilitate normalization and fold-change analysis. A *p*-value of <0.05 was considered statistically significant.

Results

EAE Scoring

Evaluation of the therapeutic effects of PEPITEM revealed that Groups G1 and G2 exhibited a steady increase in EAE scores over time, which subsequently reached a plateau. For prophylactic administration, Group G4 showed a slower and more delayed increase in EAE scores compared with Group G3, suggesting that PEPITEM may exert a preventive effect by delaying disease onset and reducing the rate of disease progression (Figs. 1,2).

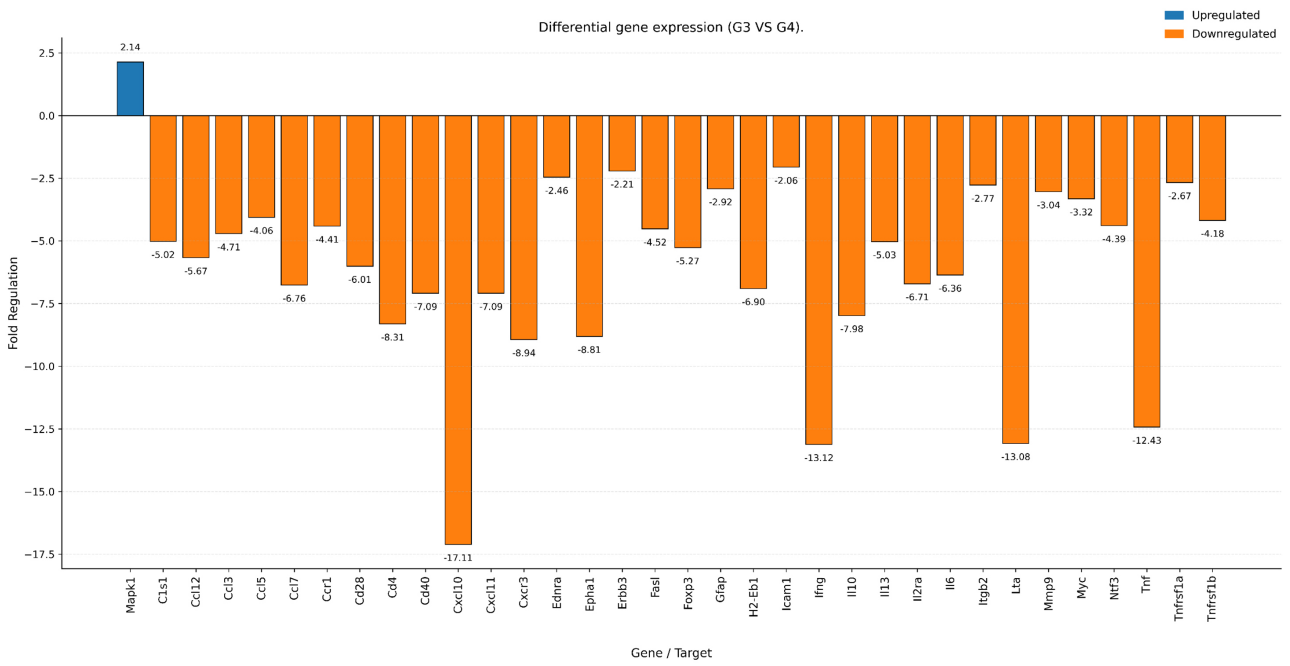

Fig. 4. Differential gene expression under prophylactic conditions (G3 vs. G4). Bar plot illustrating differential gene expression under prophylactic conditions, expressed as fold regulation, in G3 vs. G4. Positive values indicate gene upregulation, whereas negative values indicate gene downregulation relative to the reference group. Upregulated genes are shown in blue, and downregulated genes are shown in orange. Fold-regulation values were calculated using the manufacturer's ΔΔCt method. Only genes with an absolute fold regulation ≥2 and a *p*-value < 0.05 were considered significantly altered and are shown in the plot (n = 3).

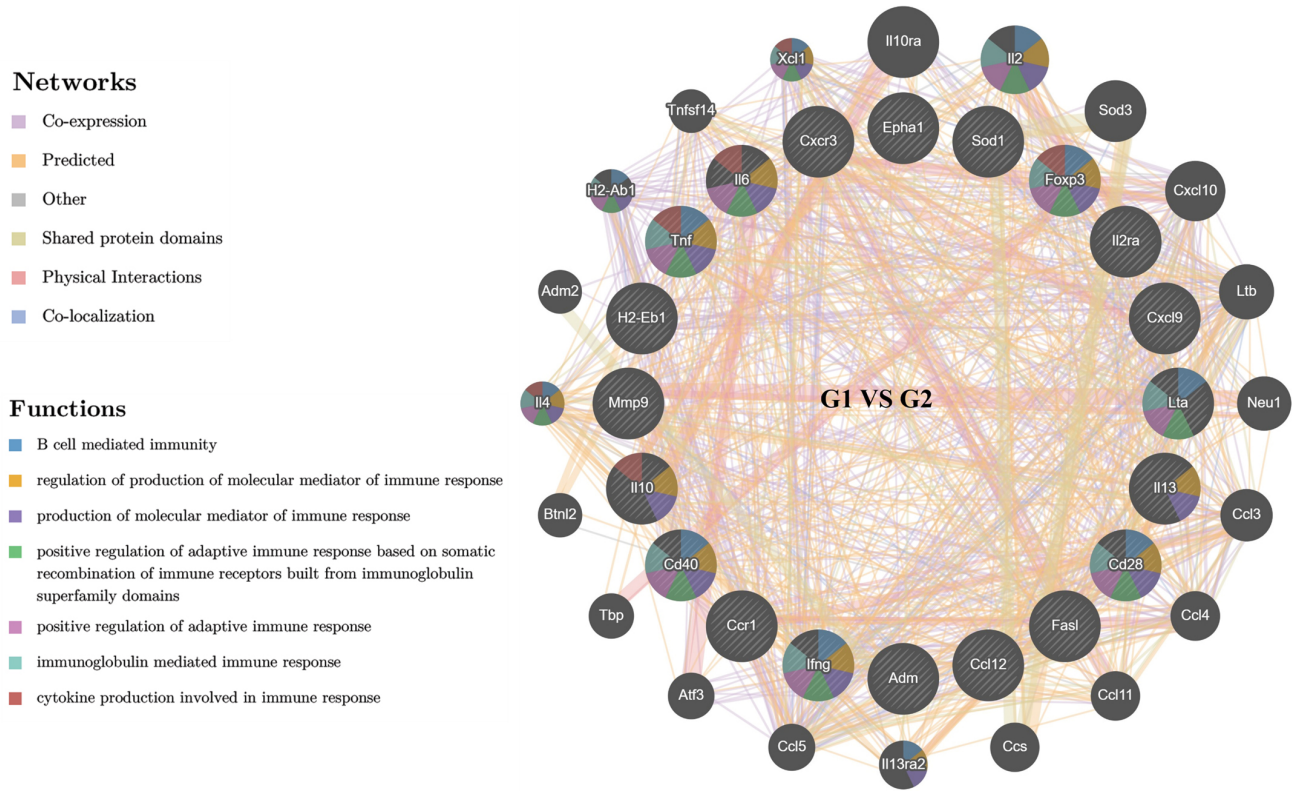

Fig. 5. *In silico* analysis of gene–gene interactions in therapeutic groups (G1 vs. G2). Network analysis depicting the relationships among differentially expressed genes in the therapeutic groups.

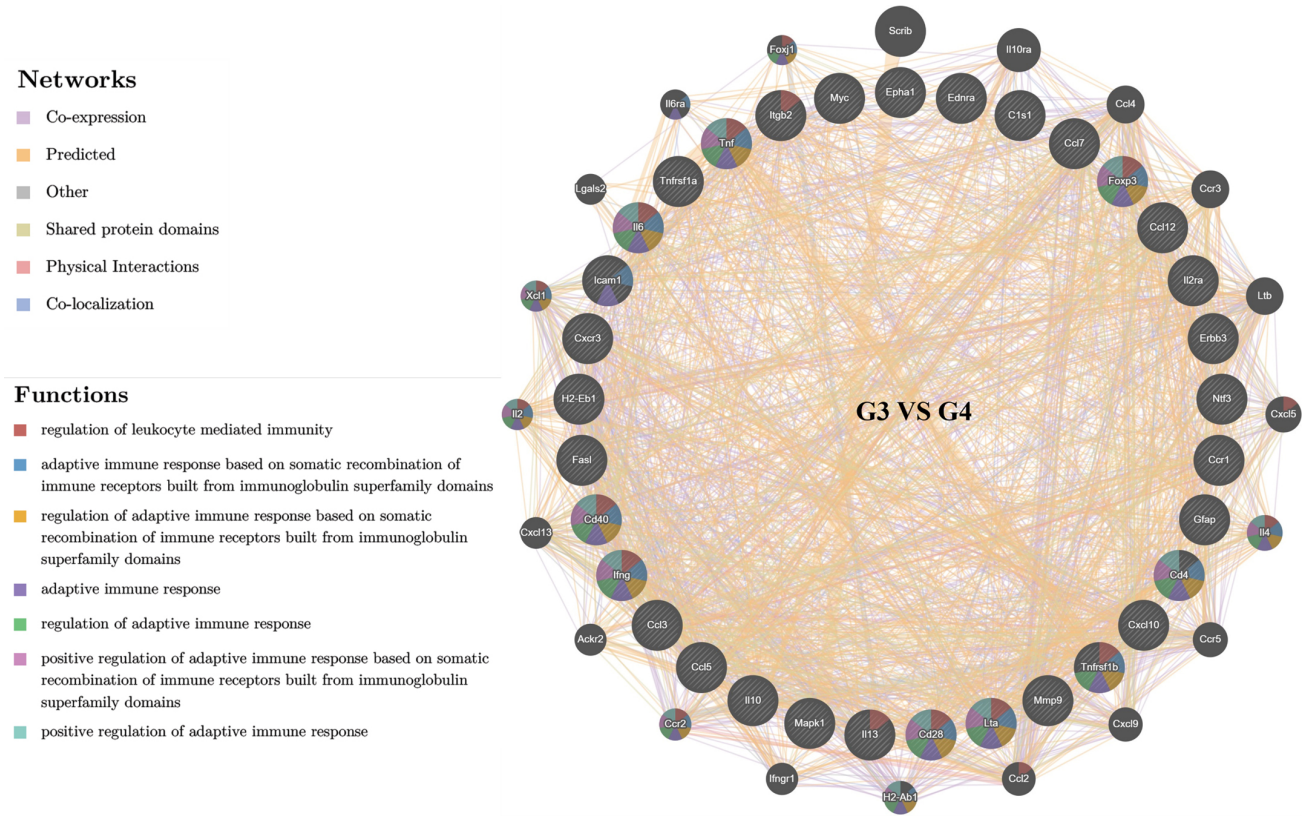

Fig. 6. *In silico* analysis of gene–gene interactions under prophylactic conditions (G3 vs. G4). Network analysis illustrating the relationships among differentially expressed genes in the prophylactic groups.

Differential Gene Expression

Differential gene expression between the therapeutic groups (G1 vs. G2) was analyzed using RT^2 Profiler™ PCR Arrays. The mean fold regulation was 10.22, indicating overall gene upregulation, whereas the median fold regulation was 4.7. The maximum fold regulation was 38.89 (corresponding to the most upregulated gene), and the minimum fold regulation was –3.79 (corresponding to the most strongly downregulated gene). Among the genes analyzed, 19 exhibited more than twofold upregulation, reflecting substantial activation by PEPITEM, whereas 2 exhibited less than 0.5-fold downregulation, indicating suppression by PEPITEM (Fig. 3).

Out of the 21 genes analyzed, 19 exhibited upregulation with a fold regulation greater than 2, while two genes were downregulated below the 0.5-fold threshold. Among the upregulated genes, *Cxcl11* (30.14-fold), *Il10* (37.9-fold), *Il13* (38.9-fold), *Lta* (29-fold), *Tnf* (15.3-fold), *Foxp3* (10.4-fold), and *Epha1* (9.5-fold) exhibited the highest fold increases, indicating a pronounced transcription response following PEPITEM treatment. Conversely, *Ccl12* (–3.79-fold) and *Sod1* (–2.04-fold) were the most strongly downregulated genes in the therapeutic condition. Additionally, functional annotation of the differentially expressed genes indicated predominant associations with chemokine signaling, cytokine–cytokine receptor interactions, and oxidative stress–related pathways, highlighting the coordinated impact of PEPITEM treatment on immune and inflammatory gene networks.

To evaluate the effect of prophylactic PEPITEM treatment on gene expression in the EAE model, differential expression was examined between the prophylactic groups (G3 vs. G4) using RT^2 Profiler™ PCR Arrays. Among the 34 genes analyzed, 33 exhibited downregulation with fold regulation values below 0.5, whereas only one gene showed upregulation above the 2-fold threshold. The most markedly downregulated genes included *Cxcl10* (–17.11-fold), *Ifng* (–13.12-fold), *Lta* (–13.08-fold), *Tnf* (–12.43-fold), and *Cxcr3* (–8.94-fold), all of which were involved in inflammatory signaling, cytokine-mediated interactions, and immune cell recruitment processes (Fig. 4).

The analysis revealed that the differentially expressed genes were primarily associated with chemokine signaling, cytokine–cytokine receptor interactions, and pathways involved in T-cell activation and migration, indicating broad transcriptional suppression of inflammatory and immune response genes. Specifically, the downregulation of *Cxcl10* suggests inhibition of immune cell trafficking, whereas the marked suppression of *Ifng*, *Lta*, and *Tnf* indicates reduced proinflammatory cytokine signaling.

In silico analysis was conducted to examine gene–gene interactions among the therapeutic (G1 vs. G2) and

prophylactic (G3 vs. G4) groups (Figs. 5,6). GeneMANIA analysis of differentially expressed genes in the therapeutic comparison (G1 vs. G2) revealed a densely interconnected immune gene network. Central nodes included multiple chemokines and cytokines (*Ccl3*, *Ccl4*, *Ccl5*, *Ccl9*, *Ccl11*, *Ccl12*, *Cxcl9*, *Cxcl10*, *Tnf*, *Ifng*, *Il2*, *Il4*, *Il6*, *Il10*, *Il13*), costimulatory and regulatory molecules (*Cd28*, *Cd40*, *Btnl2*, *Foxp3*), and trafficking- or matrix-remodeling–related genes (*Ccr1*, *Cxcr3*, *Mmp9*, *Epha1*). Functional annotation indicated significant enrichment of Gene Ontology (GO) terms associated with B cell-mediated immunity, immunoglobulin-mediated immune responses, cytokine production, and positive regulation of adaptive immune responses, consistent with coordinated activation of peripheral immune pathways. The dense network of co-expression, predicted interactions, physical protein–protein interactions, and shared protein domains among the implicated genes indicates that EAE-associated transcriptional changes occur within coordinated immune modules rather than as isolated single-gene effects.

In the comparison between G3 and G4, GeneMANIA network analysis revealed an immune-focused gene network characterized by a broader suppression of inflammatory signaling in the prophylactic PEPITEM group. Central nodes included multiple chemokines, cytokines, their receptors, and adhesion- or trafficking-related molecules, indicating that genes involved in leukocyte recruitment and activation are highly interconnected. KEGG and GO enrichment analyses identified pathways associated with chemokine signaling, cytokine–cytokine receptor interactions, and T cell-mediated immune responses. The predominance of downregulated nodes in the prophylactic group suggests that early PEPITEM administration exerts a more global dampening effect on these inflammatory gene modules than the therapeutic regimen.

Discussion

This study evaluated the effects of PEPITEM treatment in an EAE mouse model of MS by comparing therapeutic (postinduction) and prophylactic (preinduction) administration. Gene expression analysis revealed distinct transcriptional responses depending on the timing of PEPITEM administration. In the therapeutic groups (G1 vs. G2), where PEPITEM was administered after disease induction, widespread upregulation of immune-related genes was observed, with 19 of 21 genes exhibiting fold-regulation values greater than 2. Notably, *Il13* (38.9-fold), *Il10* (37.8-fold), *Cxcl11* (30.14-fold), *Cd28* (3.83-fold), and *Cd40* (3.81-fold) were among the most upregulated, indicating enhanced T-cell costimulation, chemokine signaling, and immune activation [19,20]. These findings suggest that therapeutic PEPITEM treatment may enhance immune response pathways, potentially contributing to shifts in immune cell activation and trafficking in response to ongoing neuroinflammation. Conversely, *Ccl12* (–3.79-fold) and *Sod1* (–2.04-fold) were downregulated. Downregulation of *Ccl12*, a CCR2 ligand critical for monocyte recruitment, is consistent with reduced chemokine-mediated neuroinflammation. The downregulation of *Sod1*, an antioxidant enzyme typically upregulated in EAE lesions in response to oxidative stress, was lower in the treated group; this may reflect a reduced requirement for compensatory antioxidant responses in a less inflamed CNS rather than a direct suppression of antioxidant capacity [21–23].

Regarding prophylactic PEPITEM administration (G3 vs. G4), treatment resulted in widespread suppression of inflammatory gene expression, with 33 of 34 genes significantly downregulated and only 1 gene exhibiting fold regulation above the 2-fold threshold. The most downregulated genes included *Cxcl10* (–17.11-fold), *Ifng* (–13.12-fold), *Lta* (–13.08-fold), *Tnf* (–12.43-fold), and *Cxcr3* (–8.94-fold), all of which are key mediators of proinflammatory cytokine signaling, chemokine-driven immune cell migration, and T-cell activation [24–26]. These findings are consistent with previous research reporting the therapeutic efficacy of PEPITEM in EAE [9], where early administration delayed disease onset, reduced clinical severity, and inhibited CNS leukocyte infiltration, particularly of T cells and monocytes. In this study, RT^2 Profiler™ PCR Array analysis confirmed significant downregulation of key inflammatory mediators involved in chemokine signaling and T-cell migration. Specifically, *Cxcl10*, *Ifng*, and *Tnf* were markedly suppressed, consistent with reduced immune cell recruitment and activation. These molecular alterations provide a mechanistic basis for the previously observed reduction in leukocyte infiltration and support the conclusion that prophylactic PEPITEM exerts its immunomodulatory effects through the early inhibition of proinflammatory signaling pathways. Overall, the results of this study reinforce the potential of prophylactic PEPITEM as a strategy to modulate immune responses and mitigate neuroinflammation in MS models. The data suggest that early PEPITEM administration strongly suppresses immune activation and inflammatory responses at the genetic level. This pattern contrasts sharply with therapeutic PEPITEM administration, which predominantly induced gene upregulation rather than suppression, highlighting the critical influence of intervention timing on immunomodulatory outcomes. The differential response between therapeutic and prophylactic PEPITEM treatments suggests distinct underlying mechanisms. Therapeutic PEPITEM appears to activate immune-related pathways, potentially supporting immune regulation and recovery during ongoing disease, whereas prophylactic PEPITEM broadly suppresses inflammatory genes, likely preventing excessive immune activation during the early disease stages [27,28]. Notably, the marked downregulation of *Ifng* and *Tnf* in the prophylactic group indicates that PEPITEM may dampen proinflammatory Th1 signaling, a central driver of EAE pathogenesis and MS pro-

gression [29]. Suppression of *Cxcr3* and *Cxcl10* further indicates that PEPITEM reduced immune cell infiltration into the CNS, thereby limiting neuroinflammatory damage in EAE and MS [30]. Conversely, the upregulation of *Cd28* and *Cd40* in the therapeutic group may reflect an altered T-cell activation state, potentially representing an adaptive attempt to restore immune homeostasis during disease progression [15].

Collectively, these findings indicate that PEPITEM exerts a context-dependent immunomodulatory effect, promoting immune activation when administered therapeutically postinduction but broadly suppressing inflammatory signaling when administered prophylactically. The pronounced downregulation of inflammatory genes in the prophylactic group underscores its potential to prevent disease onset, whereas the transcriptional activation observed in the therapeutic group suggests a distinct mechanism that potentially supports immune regulation and tissue repair during ongoing neuroinflammation. Future studies should examine the functional consequences of these gene expression changes at the protein level, for example, by validating key targets through Western blotting and assessing their effects on disease severity, immune cell infiltration, and clinical outcomes in EAE and MS models. This study is limited to gene expression analysis and does not confirm whether these transcriptional changes correspond to functional alterations at the protein level, highlighting the need for further validation using protein-based assays, such as Western blotting or ELISA. Furthermore, while the findings indicate the immunomodulatory effects of PEPITEM, direct assessments of immune cell dynamics and disease severity were not performed, which constrained the mechanistic interpretation of the findings.

Conclusion

PEPITEM modulates immune-related gene expression in a timing-dependent manner in EAE. Its dual effects—enhancing immune activation when administered therapeutically postinduction and broadly suppressing inflammatory pathways when given prophylactically—highlight its potential as a context-specific immunomodulatory strategy for MS.

Availability of Data and Materials

The data presented in this study are available on a reasonable request from the corresponding author.

Author Contributions

MAlassi, ASA and MLA conceptualized the idea, planned the study, contributed to the experiments, and analyses. MAlan, MAlasse, BMA, HA, AA, JS, FAS, contributed to design of experiments, sample preparation, experiments, data collection, analyses, and verification of analytical methods. All authors discussed the results, contributed to the drafting and critical revision of the manuscript, and read and approved the final draft of the manuscript. All authors have participated sufficiently in the work to take public responsibility for appropriate portions of the content and agreed to be accountable for all aspects of the work in ensuring that questions related to its accuracy or integrity.

Ethics Approval and Consent to Participate

The study was approved by the Institutional Animal Care and Use Committee (IACUC) at King Abdullah International Medical Research Center (KAIMRC) (RC-19/084/R) and by the Research Ethics Committee at King Saud University (KSU) (KSU-SE-19-10).

Acknowledgment

The authors would like to thank KAIMRC for funding this research and all KAIMRC researchers and administrative staff for their valuable assistance in this project. We also thank the animal facility at the Experimental Surgery Center at KSU for their unlimited support and cooperation during the drastic times during the pandemic.

Funding

This work was supported by KAIMRC (grant number RC19/084/R).

Conflict of Interest

The authors declare no conflict of interest.

References

[1] Liu R, Du S, Zhao L, Jain S, Sahay K, Rizvanov A, *et al*. Autoreactive lymphocytes in multiple sclerosis: Pathogenesis and treatment target. Frontiers in Immunology. 2022; 13: 996469. https://doi.org/10.3389/fimmu.2022.996469.

[2] Kamali AN, Noorbakhsh SM, Hamedifar H, Jadidi-Niaragh F, Yazdani R, Bautista JM, *et al*. A role for Th1-like Th17 cells in the pathogenesis of inflammatory and autoimmune disorders. Molecular Immunology. 2019; 105: 107–115. https://doi.org/10.1016/j.molimm.2018.11.015.

[3] Zahoor I, Mir S, Giri S. Profiling Blood-Based Neural Biomarkers and Cytokines in Experimental Autoimmune Encephalomyelitis Model of Multiple Sclerosis Using Single-Molecule Array Technology. International Journal of Molecular Sciences. 2025; 26: 3258. https://doi.org/10.3390/ijms26073258.

[4] Barry B, Erwin AA, Stevens J, Tornatore C. Fingolimod Rebound: A Review of the Clinical Experience and Management Considerations. Neurology and Therapy. 2019; 8: 241–250. https://doi.org/10.1007/s40120-019-00160-9.

[5] Galota F, Marcheselli S, De Biasi S, Gibellini L, Vitetta F, Fiore A, *et al*. Impact of High-Efficacy Therapies for Multiple Sclerosis on B Cells. Cells. 2025; 14: 606. https://doi.org/10.3390/cells14080606.

[6] Chimen M, McGettrick HM, Apta B, Kuravi SJ, Yates CM, Kennedy A, *et al*. Homeostatic regulation of T cell trafficking by a B cell-derived peptide is impaired in autoimmune and chronic inflammatory disease. Nature Medicine. 2015; 21: 467–475. https://doi.org/10.1038/nm.3842.

[7] Pezhman L, Hopkin SJ, Begum J, Heising S, Nasteska D, Wahid M, *et al*. PEPITEM modulates leukocyte trafficking to reduce obesity-induced inflammation. Clinical and Experimental Immunology. 2023; 212: 1–10. https://doi.org/10.1093/cei/uxad022.

[8] Alassiri M, Al Sufiani F, Aljohi M, Alanazi A, Alhazmi AS, Alrfaei BM, *et al*. PEPITEM Treatment Ameliorates EAE in Mice by Reducing CNS Inflammation, Leukocyte Infiltration, Demyelination, and Proinflammatory Cytokine Production. International Journal of Molecular Sciences. 2023; 24: 17243. https://doi.org/10.3390/ijms242417243.

[9] Alassiri M, Al Sufiani F, Aljohi M, Alanazi A, Alhazmi AS, Alrfaei BM, *et al*. Prophylactic administration of PEPITEM in experimental autoimmune encephalomyelitis delays disease onset, inhibits leukocyte infiltration, and alleviates severity. International Journal of Clinical and Experimental Pathology. 2024; 17: 492–505. https://doi.org/10.62347/LTAO2386.

[10] Lewis JW, Frost K, Neag G, Wahid M, Finlay M, Northall EH, *et al*. Therapeutic avenues in bone repair: Harnessing an anabolic osteopeptide, PEPITEM, to boost bone growth and prevent bone loss. Cell Reports. Medicine. 2024; 5: 101574. https://doi.org/10.1016/j.xcrm.2024.101574.

[11] Alassiri M. Therapeutic modulation of neuroinflammatory and apoptotic pathways by PEPITEM in an EAE model of multiple sclerosis. Trends in Immunotherapy 2024; 8: 6879. https://doi.org/10.24294/ti.v8.i2.6879.

[12] Dhaiban S, Al-Ani M, Elemam NM, Maghazachi AA. Targeting Chemokines and Chemokine Receptors in Multiple Sclerosis and Experimental Autoimmune Encephalomyelitis. Journal of Inflammation Research. 2020; 13: 619–633. https://doi.org/10.2147/JIR.S270872.

[13] Arimitsu NN, Witkowska A, Ohashi A, Miyabe C, Miyabe Y. Chemokines as therapeutic targets for multiple sclerosis: a spatial and chronological perspective. Frontiers in Immunology. 2025; 16: 1547256. https://doi.org/10.3389/fimmu.2025.1547256.

[14] Mazziotti V, Crescenzo F, Turano E, Guandalini M, Bertolazzo M, Ziccardi S, *et al*. The contribution of tumor necrosis factor to multiple sclerosis: a possible role in progression independent of relapse? Journal of Neuroinflammation. 2024; 21: 209. https://doi.org/10.1186/s12974-024-03193-6.

[15] Vermersch P, Wagner D, Mars LT, Noelle R, Giovannoni G. Inhibiting CD40 Ligand in Multiple Sclerosis: A Review of Emerging Therapeutic Potential. Current Treatment Options in Neurology. 2025; 27: 7.

[16] Cheng W, Chen G. Chemokines and chemokine receptors in multiple sclerosis. Mediators of Inflammation. 2014; 2014: 659206. https://doi.org/10.1155/2014/659206.

[17] Cui LY, Chu SF, Chen NH. The role of chemokines and chemokine receptors in multiple sclerosis. International Immunopharmacology. 2020; 83: 106314. https://doi.org/10.1016/j.intimp.2020.106314.

[18] Almalki E, Al-Amri A, Alrashed R, Al-Zharani M, Semlali A. The Curcumin Analog PAC Is a Potential Solution for the Treatment of Triple-Negative Breast Cancer by Modulating the Gene Expression of DNA Repair Pathways. International Journal of Molecular Sciences. 2023; 24: 9649. https://doi.org/10.3390/ijms24119649.

[19] Mado H, Stasiniewicz A, Adamczyk-Sowa M, Sowa P. Selected Interleukins Relevant to Multiple Sclerosis: New Directions, Potential Targets and Therapeutic Perspectives. International Journal of Molecular Sciences. 2024; 25: 10931. https://doi.org/10.3390/ijms252010931.

[20] Callahan V, Hawks S, Crawford MA, Lehman CW, Morrison HA, Ivester HM, *et al*. The Pro-Inflammatory Chemokines CXCL9, CXCL10 and CXCL11 Are Upregulated Following SARS-CoV-2 Infection in an AKT-Dependent Manner. Viruses. 2021; 13: 1062. https://doi.org/10.3390/v13061062.

[21] Gyoneva S, Ransohoff RM. Inflammatory reaction after traumatic brain injury: therapeutic potential of targeting cell-cell communication by chemokines. Trends in Pharmacological Sciences. 2015; 36: 471–480. https://doi.org/10.1016/j.tips.2015.04.003.

[22] Banisor I, Leist TP, Kalman B. Involvement of beta-chemokines in the development of inflammatory demyelination. Journal of Neuroinflammation. 2005; 2: 7. https://doi.org/10.1186/1742-2094-2-7.

[23] Moezzi D, Dong Y, Jain RW, Lozinski BM, Ghorbani S, D'Mello C, *et al*. Expression of antioxidant enzymes in lesions of multiple sclerosis and its models. Scientific Reports. 2022; 12: 12761. https://doi.org/10.1038/s41598-022-16840-w.

[24] Tokunaga R, Zhang W, Naseem M, Puccini A, Berger MD, Soni S, *et al*. CXCL9, CXCL10, CXCL11/CXCR3 axis for immune activation - A target for novel cancer therapy. Cancer Treatment Reviews. 2018; 63: 40–47. https://doi.org/10.1016/j.ctrv.2017.11.007.

[25] Karin N. CXCR3 Ligands in Cancer and Autoimmunity, Chemoattraction of Effector T Cells, and Beyond. Frontiers in Immunology. 2020; 11: 976. https://doi.org/10.3389/fimmu.2020.00976.

[26] Dillemans L, Yu K, De Zutter A, Noppen S, Gouwy M, Berghmans N, *et al*. Natural carboxyterminal truncation of human CXCL10 attenuates glycosaminoglycan binding, CXCR3A signaling and lymphocyte chemotaxis, while retaining angiostatic activity. Cell Communication and Signaling: CCS. 2024; 22: 94. https://doi.org/10.1186/s12964-023-01453-1.

[27] Khan Z, Mehan S, Gupta GD, Narula AS. Immune System Dysregulation in the Progression of Multiple Sclerosis: Molecular Insights and Therapeutic Implications. Neuroscience. 2024; 548: 9–26. https://doi.org/10.1016/j.neuroscience.2024.04.004.

[28] Afzali AM, Korn T. The role of the adaptive immune system in the initiation and persistence of multiple sclerosis. Seminars in Immunology. 2025; 78: 101947. https://doi.org/10.1016/j.smim.2025.101947.

[29] Furiati SC, Catarino JS, Silva MV, Silva RF, Estevam RB, Teodoro RB, *et al*. Th1, Th17, and Treg Responses are Differently Modulated by TNF-α Inhibitors and Methotrexate in Psoriasis Patients. Scientific Reports. 2019; 9: 7526. https://doi.org/10.1038/s41598-019-43899-9.

[30] Müller M, Carter SL, Hofer MJ, Manders P, Getts DR, Getts MT, *et al*. CXCR3 signaling reduces the severity of experimental autoimmune encephalomyelitis by controlling the parenchymal distribution of effector and regulatory T cells in the central nervous system. Journal of Immunology (Baltimore, Md.: 1950). 2007; 179: 2774–2786. https://doi.org/10.4049/jimmunol.179.5.2774.